Synthesis, characterization and stability of phosphonium phenolate zwitterions derived from a (diphenylphosphino)phenol derivative and oxiranes

Matthias R. Steiner [1,2] ● Christoph Marschner [3] ● Judith Baumgartner [3] ● Johann A. Hlina [4] ● Christian Slugovc *,[1,2]

[1] Institute for Chemistry and Technology of Materials, Graz University of Technology, Graz, Austria; email: slugovc@tugraz.at

[2] Christian Doppler Laboratory for Organocatalysis in Polymerization, Graz, Austria

[3] Institute of Inorganic Chemistry, Graz University of Technology, Graz, Austria

[4] Institute of Chemistry, Inorganic Chemistry, University of Graz, Graz, Austria
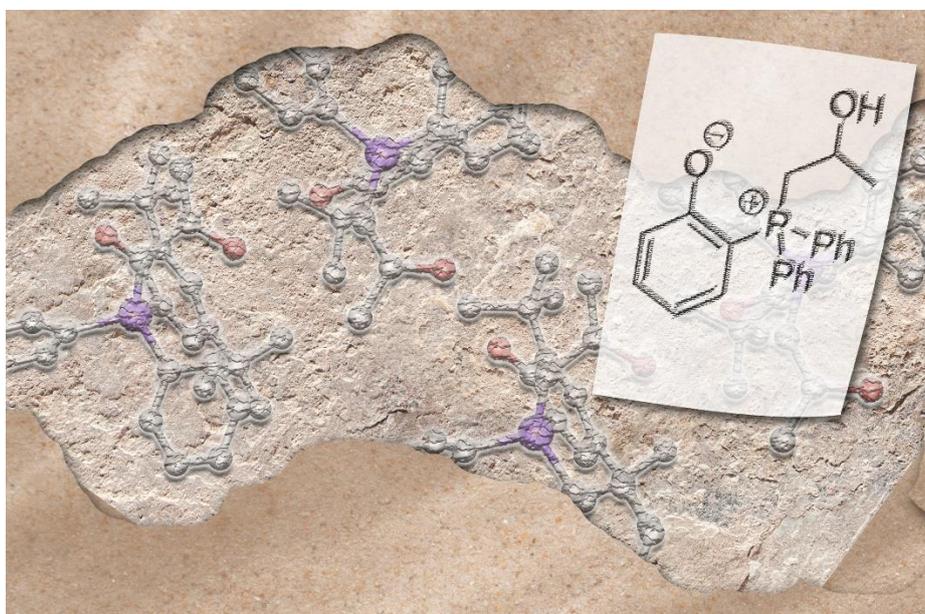
Abstract

Phosphonium phenolate zwitterions have been synthesized from 2,4-di-tert-butyl-6-(diphenylphosphino)phenol and five different oxirane derivatives. The reaction does not proceed at a detectable rate when the two reactants are combined in dichloromethane at room temperature. Despite the substantial ring strain, the reaction proceeds only with the addition of methanol, which acts as a hydrogen transfer shuttle, allowing a slow conversion to the desired zwitterions. The compounds have been fully characterized and single crystal X-ray crystallography has been performed on the methyloxirane and the phenyl glycidyl ether-derived zwitterion. The phosphonium phenolate units exhibit an ylidic bonding situation as evidenced by spectroscopic and crystallographic analysis. Glycidyl ethers were found to react faster than alkyl and aryloxiranes. Decomposition studies of the zwitterions showed high thermal stability in solution under ambient conditions. Under forced conditions (150 °C, 6 h), decomposition to the corresponding phosphine oxide and secondary aliphatic alcohols, the formally hydrogenated oxirane derivative, was observed.

Introduction

Epoxy molding compounds used to protect semiconductor circuits from environmental factors such as moisture, heat, and shock are typically based on diglycidyl ethers of various bisphenol A derivatives and so-called phenol-aralkyl resins, which are products of the condensation reaction between aldehydes and alkylphenols, as hardeners. In addition, additives and fillers are used, and an important component is the so-called accelerator, which accelerates the curing of the resin typically at temperatures above 150 °C and increases the number of molding cycles for mass production [1,2,3,4,5]. In particular, triarylphosphine accelerated formulations have optimal physical properties when cured, which subsequently improves the reliability of the encapsulated semiconductors [6,7,8,9] and recent work is attempting to further improve their properties [10,11,12]. Mechanistically, the accelerated curing of the epoxy-phenol reaction is explained by the initial formation of betaine I (Scheme 1) by nucleophilic attack of the phosphine from the side opposite to the oxygen of the oxirane group onto the sterically less hindered carbon atom of the oxirane ring. In turn, the Brønsted-basic zwitterion I undergoes an acid-base reaction with the phenols to form ion pair II. The resulting phenolates are more reactive with epoxy groups than phenols, which explains the faster curing. [1-4].
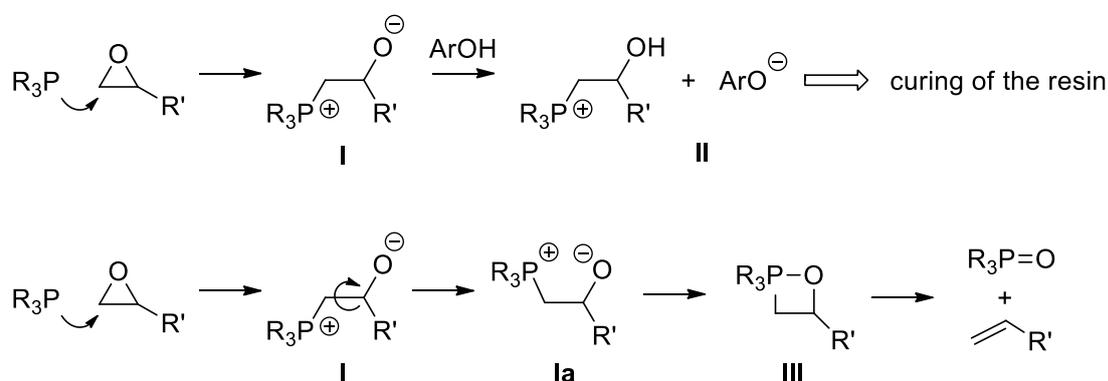
Scheme 1. The reaction of phosphines with epoxides resulting in the curing of epoxy-phenol formulations (above) and in phosphine oxides and alkenes (below)

Apparently, tertiary aromatic phosphines work as intended in these formulations, although it has long been known that epoxides and tertiary phosphines react to give the corresponding deoxygenated alkene and phosphine oxide as products [13,14,15]. The reaction mechanism has been studied theoretically [16] and catalyzed versions of the reaction have been disclosed [17,18,19]. The overall reaction is described by four steps and starts with the phosphine's attack of the oxirane forming the same zwitterionic structure I as in the first step of the epoxy phenol reaction (Scheme 1). In a next step, the betaine I is transformed by rotation into the betaine Ia, which then forms the oxaphosphetane derivative III. Finally III decomposes to release the end-products, the corresponding phosphine oxide and the alkene.

Here we would like to report our contribution to a better understanding of the reaction of epoxides with phosphines. We have chosen a (diphenylphosphino)phenol derivative combining the phenol and the phosphine into a single molecule [20] to study in particular the first step of the reaction and found evidence for the elusive formation of phosphonium phenolate species reminiscent of II. The resulting zwitterionic molecules do not undergo the deoxygenation reaction and are thermally quite stable, making them potentially interesting as catalysts for various reactions such as the synthesis of cyclic carbonates from epoxides and CO_2 [21,22] or organophotoredox catalysis [23,24].

Results and Discussion

First we tested triphenylphosphine (PPh$_3$) and 2,4-di-*tert*-butyl-6-(diphenylphosphino)phenol (**1**) as initiators for the homopolymerization of phenyl glycidyl ether (PGE). 4-(Dimethylamino)pyridine (DMAP) was used as a benchmark and the activity of the initiators (5 mol% with respect to PGE) was investigated by dynamic differential scanning calorimetry (DSC) accompanied by on-line monitoring of sample weights in a simultaneous thermal analysis (STA) instrument. The results are shown in Figure 1.
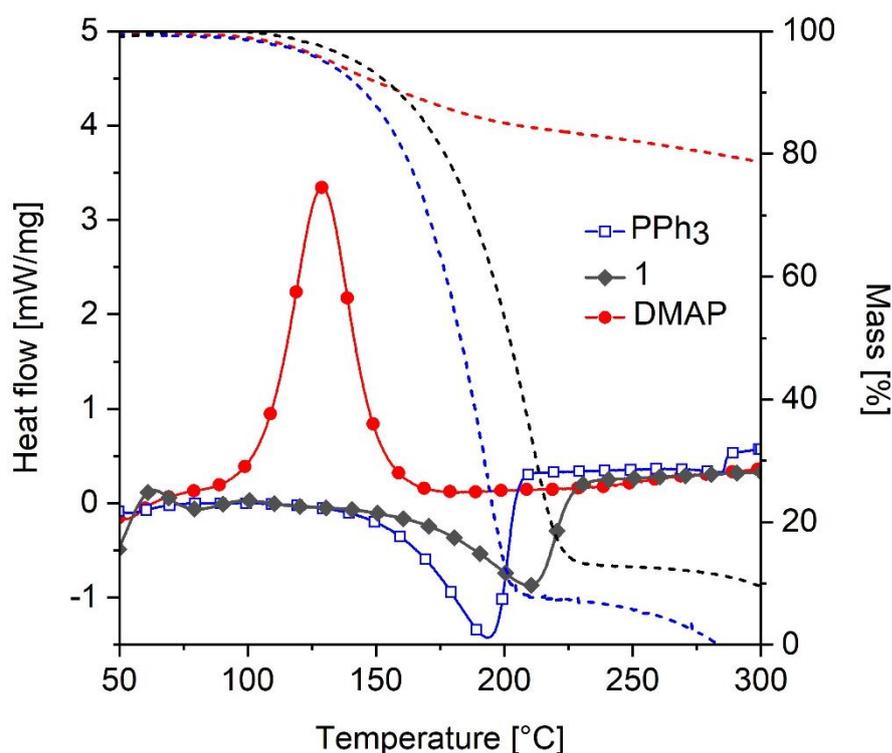

*Figure 1. Dynamic STA measurements of the homopolymerization of PGE initiated with DMAP, PPh$_3$ and **1** (5 mol% in respect to PGE; heat rate = 10 K min^{-1}) showing the heat flow of DSC experiments (thick lines with symbols, exothermal reactions show a positive heat flow) and the masses of the samples in dependence of the temperature (dashed lines with the same color code).*

In the DMAP case, an onset of the polymerization was observed at about 80 °C. The reaction showed its maximum heat flow at 129 ± 1 °C and a heat of polymerization of about 96 ± 3 kJ mol^{-1} was determined. At 210 °C a mass loss of $16 \pm 2\%$ was observed, which was attributed to the evaporation of PGE not yet incorporated into the macromolecules [25]. In the case of PPh$_3$ no heat of polymerization could be observed, but only the evaporation of PGE as evidenced by the endothermic heat flow signal peaking at 193 °C and the pronounced mass loss resulting in about 7 % residual mass at 230°C. With **1** as the initiator, less mass loss (about 13% residual mass at 230 °C) and a less pronounced endothermic heat flow with a peak at a higher temperature (209 °C) were observed than in the case of PPh$_3$. Accordingly, both phosphines are not well suited to initiate the homopolymerization of PGE under these conditions.

In a next step, we investigated the reaction of PGE with 5 mol% of the phosphines at room temperature and 80 °C. In each case, no polymerization of PGE could be detected after 24 h and most of the PGE remained unreacted. For the reaction with PPh$_3$ at room temperature, two thirds of the PPh$_3$ was still present in the reaction mixture and one third was oxidized to triphenylphosphine oxide (OPPh$_3$), as revealed by ^{31}P-NMR spectroscopy (see Figs. S2). Small amounts of (allyloxy)benzene were observed in the proton NMR spectrum ((allyloxy)benzene was identified by comparison to published NMR data [26]). At 80 °C PPh$_3$ was fully converted to OPPh$_3$ and (allyloxy)benzene was clearly detected in the proton NMR spectrum. Integration revealed an OPPh$_3$: (allyloxy)benzene ratio of 2.5 : 1, suggesting that OPPh$_3$ was formed by direct oxidation and by the deoxygenation reaction responsible for (allyloxy)benzene formation. In contrast, no (allyloxy)benzene was detected with **1** as the phosphine. After 24 h at room temperature, 74 % of **1** was still present and only 7 % of the corresponding phosphine oxide was found [27]. In addition, a previously unknown peak appeared which accounted for 19 % of the phosphine signals. At 80 °C, about 80 % of this unknown substance formed together with about 8 % of the oxide of **1** and several unknown phosphorus signals (12 % in total; see Fig. S10).

As a next step, we sought to isolate and identify the unknown main product, which we hypothesized to be the corresponding phosphonium phenolate zwitterion resulting from the ring opening of PGE by **1** followed by hydrogen transfer. Similar zwitterionic species have been prepared by reaction of **1** with Michael acceptors [28], and we anticipated a similar reactivity with epoxides. In case of using epoxides, the reaction is additionally driven by the release of the ring strain (about 27 kcal/mol) [29,30]. However, when **1** was reacted with PGE at ambient conditions in dichloromethane (1.3 mmol/dm^3) no conversion to the above detected species was observed over one week. Drawing parallels to the formation of zwitterions with Michael acceptors [28], the lack of reactivity is likely due to hindered hydrogen transfer from the phenol derivative **1** to the alkoxide in I (see Scheme 1). Accordingly, 5 equivalents of methanol were added to the reaction mixture and slow formation of the desired product was observed at room temperature. Amongst PGE, methyloxiran, ethyloxiran, phenyloxiran and

p.4

(butoxymethyl)oxirane were also used as substrates and in all cases the addition of methanol was necessary to achieve conversion to the desired products (Scheme 2). In general, the reaction rate is low and a quantitative conversion of **1** cannot be achieved within a week at room temperature. No by-product formation has been observed under these conditions. Therefore, a typical preparation of the zwitterions is carried out at room temperature using the lowest possible dilution (solvent dichloromethane with methanol) for 7 days. The remaining starting materials are then separated by recrystallization, resulting in moderate (non optimized) yields of the zwitterions **2a**-**2e** (see Table 1).
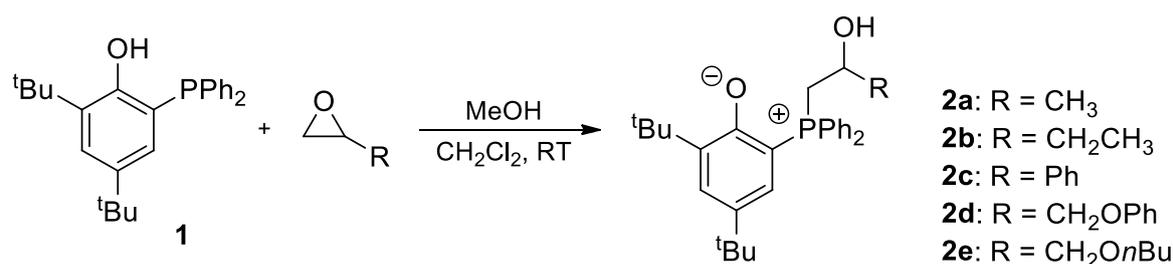
*Scheme 2. Reaction of **1** with different epoxies, forming the zwitterions **2a**-**2e***

The compounds were characterized by ^{1}H, ^{13}C and ^{31}P NMR spectroscopy and the final proof of the molecular structure was obtained by single crystal X-ray structure determination (vide infra). In the ^{1}H-NMR spectrum, a characteristic doublet of doublets signal is observed in the range of 6.10 to 6.15 ppm for the zwitterions **2a**-**2e** (see Table 1). This resonance is attributed to the proton at position 5 in the 2,4-di-*tert*-butylphenolate substituent of the zwitterions and undergoes meta-coupling to the proton at position 3 ($^4J_{HH} \approx 2.5$ Hz) as well as coupling to phosphorus ($^3J_{PH} \approx 14.5$ Hz). For comparison, the same proton in the parent phosphine **1** shows a resonance at 6.88 ppm [31]. In the Michael acceptor-derived zwitterions, this proton is similarly shifted upfield as in **2a**-**2e** and is found in the range of 6.09 to 6.21 ppm [28].

*Table 1. Yield and characteristic chemical NMR-shifts for zwitterions **2a**-**2e***

Number	R	Yield [%]	^{1}H-NMR shift of Ph^5 [ppm]	^{13}C-NMR shift of Ph^1 [ppm]	^{13}C-NMR shift of Ph^6 [ppm]	^{31}P-NMR shift [ppm]
2a	CH$_3$	64	6.10	172.8	100.9	18.3
2b	CH$_2$CH$_3$	36	6.04	173.7	100.3	18.8
2c	Ph	48	6.15	173.6	100.4	18.3
2d	CH$_2$OPh	59	6.12	173.4	100.7	18.7
2e	CH$_2$O*n*Bu	34	6.04	173.6	100.7	18.9

The ^{13}C NMR spectrum of **2d** is shown in Fig. 2 and is representative of all zwitterions disclosed herein. The carbon atom in position 1 of the 2,4-di-*tert*-

butylphenolate substituent shows a doublet ($^2J_{PC} \approx 4.5$ Hz) in the range of 172.8 to 173.7 ppm (Table 1), which is indicative of a quinonic resonance structure, since benzoquinones show shifts of about 188 ppm, whereas hydroquinones appear at about 150 ppm [32] (in the parent phosphine **1** the corresponding peak is observed at 155.9 ppm [31]). The most characteristic chemical shift for the zwitterions **2a**-**2e** in the ^{13}C NMR spectra is found for the resonances of carbon 6, which are observed in the range of 100.4 to 100.9 ppm ($^1J_{PC} \approx 95$ Hz). As expected, the diastereotopic phenyl substituents give rise to two distinct sets of ^{13}C signals as shown in Fig. 2. The ^{13}C chemical shifts for the methylene carbon 15 (directly attached to the phosphorus atom) are found in the range of 34.7 to 40.7 ppm ($^1J_{PC}$ between 64 and 54 Hz). For comparison, the corresponding carbon atom in similar alkyltriphenylphosphonium halides resonates at 27-18 ppm ($^1J_{PC} \approx 54$ Hz) [33,34].
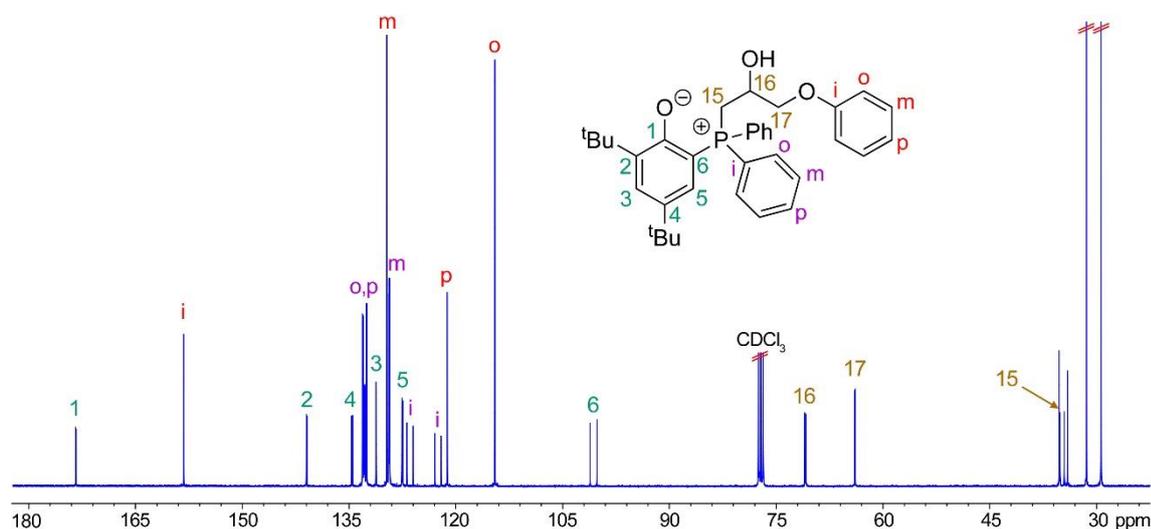

Figure 2. ^{13}C{^{1}H}-NMR spectrum of **2d** *in CDCl$_3$ recorded at 100 MHz; numbering in accordance with the numbering of the atoms in the molecular structures retrieved from single crystal X-ray measurements.*

The ^{31}P NMR shift (against H$_3$PO$_4$, 85%) of the adducts is in the range of 18.9-18.3 ppm, which is slightly shifted upfield compared to the corresponding values for the Michael acceptor derived zwitterions of **1** [28]. For comparison, the phosphine **1** has a ^{31}P NMR shift of −29.7 ppm [31].

Crystals suitable for single crystal X-Ray diffraction analysis were obtained from compounds **2a** and **2d**. Crystals of **2a** were grown from a concentrated solution in toluene/THF (3:1) and two crystallographically independent conformers of **2a** were found in the unit cell. As shown in Fig. 3, one conformer exhibits an intramolecular hydrogen bonding interaction between the phenolate oxygen (O1) and the proton of the hydroxyl group (attached to O2) resulting in an O1-O2 distance of 2.583(5) Å. The second conformer crystallizes in a hydrogen bonded coordination polymer in which the phenolate oxygen (O3) is 2.596(5) Å apart

p.6

from the oxygen atom (O4) of the hydroxyl group of the next repeating unit. In **2d**, the conformer with the intramolecular hydrogen bond was found with a O1-O2 distance of 2.519(4) Å (Fig, 2 gray box). The P1–O1 distances of 2.813(4) Å (**2a**, intramolecular hydrogen bonding) and 2.708(4) Å (**2a**, intermolecular hydrogen bonding) as well as 2.826(3) Å in **2d** suggest a weak binding interaction between the phenolate and the phosphonium center as observed in similar zwitterions with P–O distances in the range of 2.60–2.95 Å [28,35,36] (Fig. 3, ochre box). The P1-O2 distance is with 3.500(3) Å (in **2d**) or 3.313(4) Å and 3.574(4) Å (**2a** chain conformer and **2a** ring conformer) significantly higher. In any case, the P-O distances are significantly larger than expected for covalent P-O bonds in 1,2-oxaphosphetanes [37].
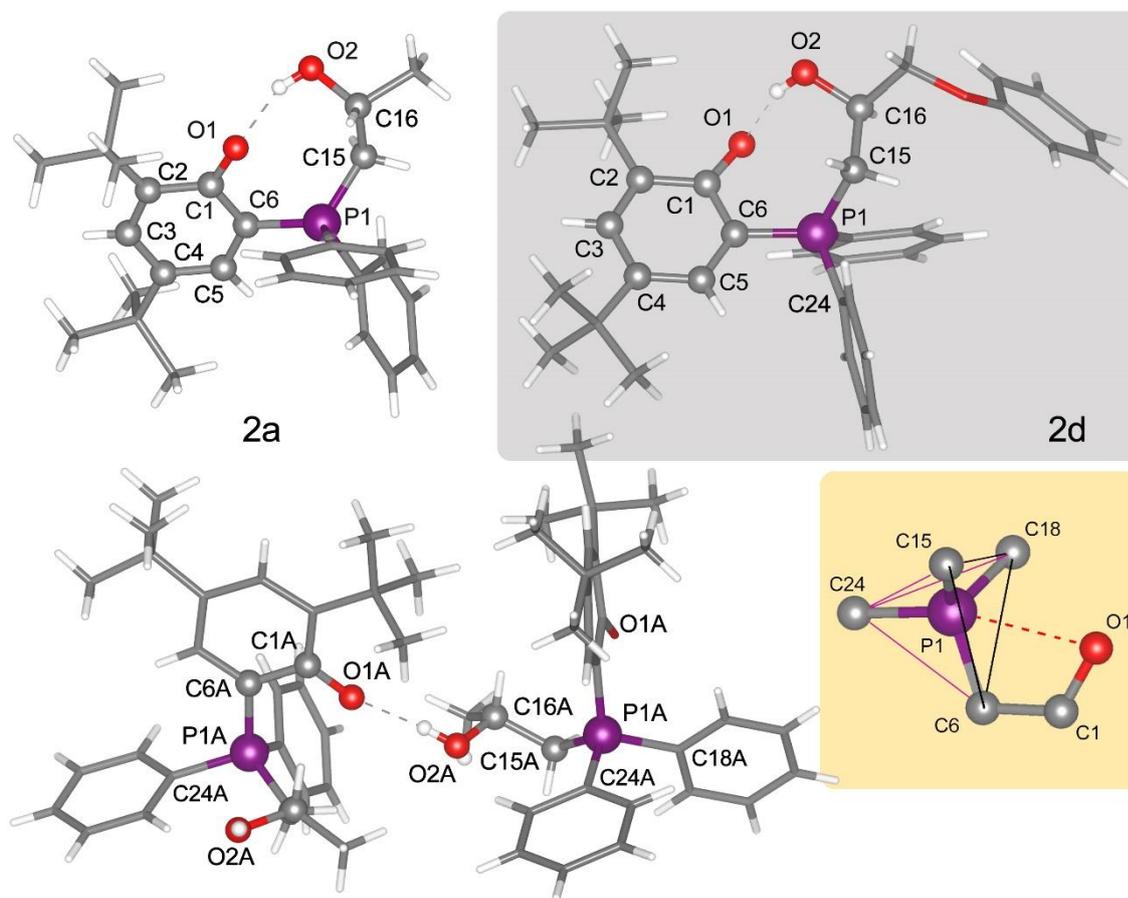
*Figure 3. Results of single crystal X-ray diffraction measurments showing the molecular structures of the two independent conformers of **2a** present in the crystal; above: intramolecular hydrogen bonding forms a 8-membered ring; below: intermolecular hydrogen bonding results in a coordination polymer and of **2d** (shown in the gray box); the sketch in ochre box illustrates the bonding situation of the phosphorous atom.*

This weak interaction of P1 and O1 causes a slight distortion of the tetrahedral bonding geometry around the phosphonium atom towards a distorted trigonal pyramidal geometry with C24 and O1 as the apexes, which can be seen by the fact

that each of the atoms C6, C15 and C18 have angles smaller than 109.5° with the atom C24 (e.g. C6-P1-C24 = 107.3(3)°, C15-P1-C24 104.3(3)°, C18-P1-C24 106.2(3)° in **2a** with intramolecular hydrogen bonding). Furthermore, the P1-C24 distance is always slightly larger than the distance between P1 and C18 (e.g. 1.825(5) Å and 1.813(5) Å in **2a** with intramolecular hydrogen bonding). Finally, the O1-P1-C18 angles are between 163° and 165°, and the torsion angle defined by O1-C1-C6-P1 is in all cases less than 7°.

The bonding situation in the phenolate ring is similar to what have been found for Michael-acceptor derived zwitterions [28] or for (triphenylphosphonium)-phenolate and point to an electron delocalization within a ylidic system [24,35]. The P1-C6 distances in **2a** (1.774(4) Å for the conformer with intramolecular hydrogen bonding and 1.780(4) Å for the intermolecular hydrogen bonded molecules) and in **2d** (1.778(4) Å) are significantly shorter than the corresponding P-C18 and P-C24 distances and shorter than in the free phosphine **1** (1.825 Å) [38]. The same accounts for the O1-C1 bond lengths, which are notably shorter in the zwitterions **2a** (1.286(5) Å and 1.292(4) Å) and **2d** (1.297(4) Å) than in the parent phosphine **1** (1.373(2) Å) [38].

All presented zwitterions exhibit similar spectral properties with a single absorption feature ranging from 310 to 410 nm, peaking at 346 ± 1 nm. The molar extinction coefficients are in between 5300 and 5800 $dm^3 \ mol^{-1} \ cm^{-1}$. Absorption spectra can be found in the supporting information (Figure S47).

In order to estimate the relative reactivity of the epoxides studied, the formation of the zwitterions **2a**-**2e** was followed over time. In contrast to the preparation of the zwitterions, we changed the amounts of reactants and used 10 equivalents of the respective epoxide and 10 equivalents of methanol (with respect to **1**). Furthermore, a defined volume of mesitylene was added as an internal standard for integrating the ^{1}H NMR spectra used to quantify the conversion after specific time intervals of the reaction carried out at room temperature. The zwitterions were formed exclusively, as no other products were observed in either the ^{1}H NMR or ^{31}P NMR spectra. The results are shown in Fig. 4 and show a faster reaction of glycidyl ethers than for methyloxirane, ethyloxirane and phenyloxirane. A similar reactivity trend was observed for epoxy-amine reactions [39].

Compound **2d** was subjected to decomposition studies in three different NMR solvents, namely benzene-d_6, $CDCl_3$ and CD_3CN. Solutions of **2d** were either stored at room temperature or heated to 60 °C and the samples were subjected to ^{1}H and ^{31}P NMR analysis after specified time frames. At room temperature, no degradation was observed in any of the solvents after 7 days.
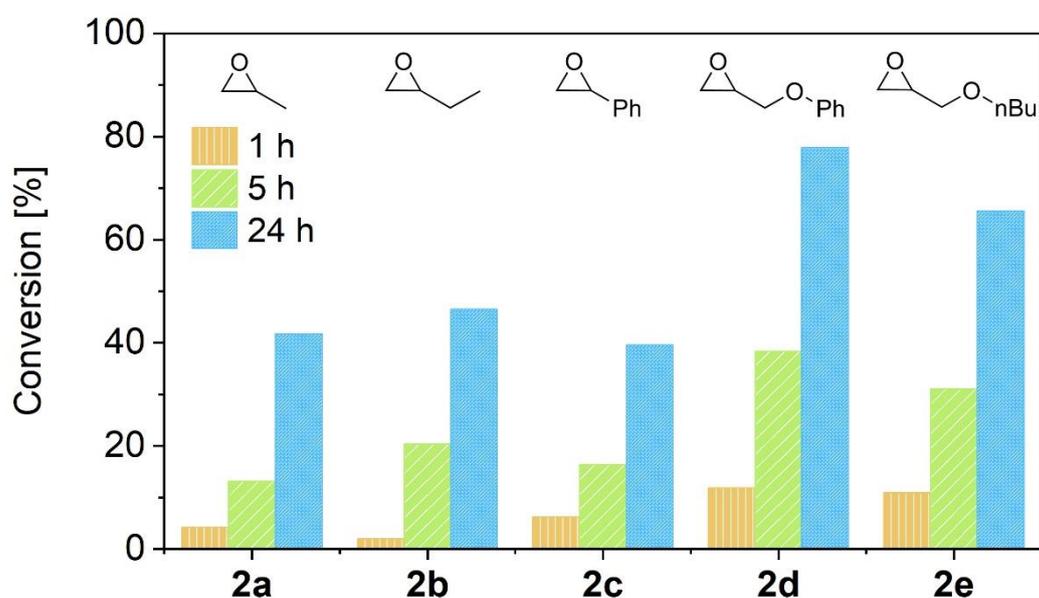
*Figure 4. Conversion of **1** into the corresponding zwitterions **2a-2e** as determined by ^{1}H NMR spectroscopy of the reaction mixture; reaction conditions: 1 equiv. **1**, 10 equiv. oxirane derivative, 10 equiv. methanol, room temperature.*

The same is true for solutions **2d** in CDCl$_3$ and CD$_3$CN stored at 60 °C for 3 d. After 7 days at 60 °C, traces of phosphine oxide are observed in the CDCl$_3$ solution, while in acetonitrile no decomposition was detected even after this time. It appears that epoxy-based phosphonium phenolate zwitterions are more stable than their Michael acceptor-derived counterparts, which already show decomposition/oxidation under similar conditions [28]. However, the benzene-d$_6$ solution shows signs of decomposition earlier. After 7 d at 60 °C, some oxide of **1** (less than 3 %) is visible in the ^{31}P NMR spectrum and new peaks (multiplets at 3.44 and 3.85 ppm) are present in the ^{1}H NMR spectrum. The characteristic ^{1}H NMR signals of (allyloxy)benzene were not observed. In an attempt to identify the newly formed species, **2d** was dissolved in CDCl$_3$ and heated to 150 °C for 6 h in an autoclave. The resulting solution was directly subjected to NMR and GC-MS analysis and the main decomposition products could be identified as phenoxypropan-2-ol and the phosphine oxide formed from **1** [40] (Scheme 3).
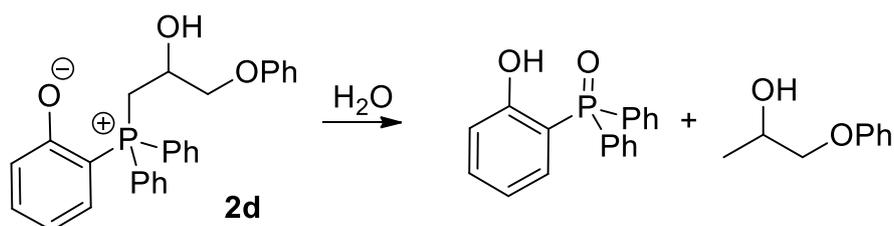
*Scheme 3. Decomposition of the zwitterion **2d***

p.9

Further decomposition products included phenol as well as other unidentified products in small amounts (in sum less than 15 %, see Figs S43 and S44). The formation of phenoxypropan-2-ol from **2d** requires a formal reduction of the 2-hydroxy-3-phenoxypropyl group and oxidation of the phosphonium to a phosphine oxide. This redox reaction may be facilitated by water, as it has long been known that tertiary phosphines and water form the corresponding phosphine oxides and hydrogen under alkaline conditions [41]. Furthermore, it has been shown that the attack of water on phosphonium centers leads to the elimination of the corresponding newly formed phosphine oxide [42]. In a recent publication, this reactivity is exploited in a photocatalytic phosphine-mediated water activation for hydrogenation of alkenes [43].

Conclusion

The reaction of 2,4-di-*tert*-butyl-6-(diphenylphosphino)phenol with various oxirane derivatives yields phosphonium phenolate zwitterions. The use of a hydrogen transfer agent, in this case methanol, is necessary to facilitate the reaction at room temperature. Therefore, it can be said that the failure of PPh$_3$ and **1** to promote the phenyl glycidyl ether homopolymerization is not due to the same degradation reaction. While PPh$_3$ deactivates via Wittig chemistry, forming (allyloxy)benzene via the intermediate initial zwitterion, this degradation pathway is blocked by the addition of phenols. The acidic phenols protonate the alkoxide group present in the initially formed zwitterion, thereby inhibiting the oxaphosphetane formation ultimatively leading to the formation of olefins and phosphine oxides. The resulting phenolate is a much weaker nucleophile than the initially formed alkoxide, which explains the high temperatures required to cure epoxy-phenol formulations compared to the DMAP initiated homopolymerization. Phosphonium phenolates, as shown here for the zwitterion **2d**, decompose via a different pathway resulting in the formation of the phosphine oxide and secondary alcohols resulting from the formal hydrogenation of the oxirane derivative.

Experimental

All experiments were performed under ambient conditions. Chemicals were purchased from Sigma-Aldrich, Carl Roth, Merck, or TCI and were used as received. 2,4-Di-*tert*-butyl-6-(diphenylphosphino)phenol (**1**) was prepared according to a published procedure [44]. NMR spectra were recorded on a Bruker AVANCE III 300 spectrometer or a JEOL JNM-ECZ 400 MHz spectrometer and are referenced to tetramethylsilane (^{1}H, ^{13}C), and 85% H$_3$PO$_4$ (^{31}P). Deuterated solvents were obtained from Cambridge Isotope Laboratories Inc. UV-Vis spectra were recorded on an Agilent Cary 60 UV-Vis spectrophotometer. Thermogravimetric analysis (TGA) and differential scanning calorimetry (DSC) was performed with a Netzsch simultaneous thermal analyzer STA 449C

p.10

(crucibles: aluminum from Netzsch). The heating rate was 10 °C/min until a final temperature of 550 °C was reached. A helium flow of 20 cm^3·min^{-1} was used in combination with a protective flow of helium of 10 cm^3·min^{-1}. Typically, 200 mg (1 eq, 1.33 mmol) of PGE were mixed with the respective initiator (0.05 eq, 0.067 mmol) until a homogeneous mixture was obtained. From this solution, 3 to 15 mg were transferred into the aluminum crucible, which was then pressed closed. A hole was cut through the lid to enable evaporation. The crucible was then subjected to the temperature program specified above. For decomposition studies, 20 mg (0.037 mmol) of **2d** were dissolved in 0.7 cm^3 of the respective deuterated solvent (CDCl$_3$, C$_6$D$_6$ or CD$_3$CN). The solution was kept in an NMR tube either at room temperature or at 60 °C and subjected to ^{1}H and ^{31}P NMR analysis after specific time frames. The decomposition study using **2d** at forcing conditions was carried out as follows: 30 mg **2d** (0.06 mmol) were dissolved in 0.7 cm^3 CDCl$_3$ and heated to 150 °C for 6 h using a Monowave 50 reactor (Anton Paar). The resulting yellow solution was then directly subjected to NMR and GC-MS analysis using an Agilent Technologies 7890A GC system equipped with an Agilent Technologies J&W HP 5MS capillary column (30 m x 0.25 mm x 0.25 µm film with 5 % phenyl- and 95 % methylpolysiloxane). He 5.0 (Air Liquide) was used as carrier gas at a constant flow rate. Samples were injected in split mode using an Agilent Technologies 7683 Series autosampler and an Agilent Technologies 7683B Series injector. Methanol and ethyl acetate were used to flush the needle before and after injection. Masses were analyzed with a 5975C mass selective detector (inert MSD with Triple Axis Detector system) by electron-impact ionization with a potential of E = 70 eV. The following temperature program was used for all GC-MS measurements: 50 °C 1 min, followed by a linear heating ramp (40 °C per minute until 300 °C) and 5 min at 300 °C, solvent delay: 4.0 min. For X-ray structure analyses the respective crystals were mounted onto the tips of glass fibres. Data collection was performed with a Bruker-AXS SMART APEX CCD diffractometer using graphite-monochromated Mo-K_α radiation (0.71073 Å). The data were reduced to F$_o$^{2} and corrected for absorption effects with SAINT (*Version 6.45, Bruker AXS Inc., 1997-2003*) and SADABS (*Version 2.10. Bruker AXS Inc.*) respectively [45]. The structures were solved by direct methods and refined by full-matrix least-squares method (SHELXL97 or SHELXL19) [46]. If not noted otherwise all non-hydrogen atoms were refined with anisotropic displacement parameters. All hydrogen atoms were located in calculated positions to correspond to standard bond lengths and angles. Figures of solid state molecular structures were generated using VESTA [47]. Crystallographic data for the structures reported in this paper have been deposited with the Cambridge Crystallographic Data Centre as supplementary publication no. CCDC 2330232 (**2a**) 2330231 (**2d**).

2,4-di-tert-butyl-6-((2-hydroxypropyl)diphenylphosphonio)phenolate (**2a**, $C_{29}H_{37}O_2P$)

Phosphine **1** (200 mg, 0.51 mmol, 1 eq) was dissolved in 2-methyloxirane (296 mg, 5.1 mmol, 10 eq) and methanol (82 mg, 2.6 mmol, 5 eq) in a 4 cm^3 screw-cap vial. The reaction mixture was stirred at room temperature for 5 days. Afterwards all volatiles were evaporated in vacuo and the residue recrystallized by vapor diffusion of pentane on a concentrated solution in THF. The crystals were filtered off, washed with pentane and dried in vacuum. Yield: 147 mg (pale yellow crystals, 64.2 %). ^1H NMR (δ in ppm, 300 MHz, $CDCl_3$, 298 K): 1.05 (s, 9H, CCH_3), 1.36-1.49 (m, 12H, CCH_3 + C(OH)-CH_3), 2.90-3.05 (m, 1H, CH_2), 3.07-3.24 (m, 1H, CH_2), 4.26-4.42 (m, 1H, (OH)CH), 6.10 (dd, $^3J_{P-H}$ = 14.8 Hz, $^4J_{H-H}$ = 2.4 Hz, 1H, H5), 7.34-7.44 (m, 2H, Ar-H), 7.46 (d, 1H, $^4J_{H-H}$ = 2.4 Hz, H3), 7.48-7.57 (m, 6H, Ar-H), 7.58-7.67 (m, 2H, Ar-H). $^{13}C\{^1H\}$ NMR (δ in ppm, 75 MHz, $CDCl_3$, 298 K): 25.2 (d, $^3J_{P-C}$ = 17.3 Hz, (OH)CCH_3), 29.4 (s, CCH_3), 31.4 (s, CCH_3), 34.1 (d, $^4J_{P-C}$ = 1.2 Hz, CCH$_3$), 35.3 (d, $^4J_{P-C}$ = 2.1 Hz, CCH$_3$), 39.2 (d, $^1J_{P-C}$ = 63.9 Hz, PCH$_2$), 61.4 (d, $^2J_{P-C}$ = 4.7 Hz, (OH)C), 100.9 (d, $^1J_{P-C}$ = 96.5 Hz, C6), 122.8 (d, $^1J_{P-C}$ = 88.3 Hz, C$_{i-Ph}$), 126.4 (d, $^1J_{P-C}$ = 85.4 Hz, C$_{i-Ph}$), 127.5 (d, $^2J_{P-C}$ = 12.6 Hz, C5), 129.3 (d, $^3J_{P-C}$ = 11.0 Hz, C$_{m-Ph}$) , 129.5 (d, $^3J_{P-C}$ = 11.0 Hz, C$_{m-Ph}$), 131.1 (d, $^4J_{P-C}$ = 1.6 Hz, C3), 132.6 (d, $^2J_{P-C}$ = 8.6 Hz, C$_{o-Ph}$), 132.8 (d, $^3J_{P-C}$ = 2.8 Hz, C$_{m-Ph}$), 133.0 (d, $^2J_{P-C}$ = 9.6 Hz, C$_{o-Ph}$), 134.9 (d, $^3J_{P-C}$ = 15.0 Hz, C4), 141.1 (d, $^4J_{P-C}$ = 7.8 Hz, C2), 172.8 (d, $^2J_{P-C}$ = 4.2 Hz, C1). $^{31}P\{^1H\}$ NMR (δ in ppm, 162 MHz, $CDCl_3$, 298 K): 18.3. UV-Vis ($CHCl_3$): λ_{max} = 346 nm (ε = 5.55 * 10^3 dm^3 mol^{-1} cm^{-1}).

2,4-di-tert-butyl-6-((2-hydroxybutyl)diphenylphosphonio)phenolate (**2b**, $C_{30}H_{39}O_2P$)

Phosphine **1** (200 mg, 0.51 mmol, 1 eq) was dissolved in dichloromethane (0.3 cm^3) in a 4 mL screw-cap vial and methanol (82 mg, 2.6 mmol, 5 eq.) was added. In a separate vial, 2-ethyloxirane (37 mg, 0.51 mmol, 1 eq.) was dissolved in dichloromethane (0.1 cm^3) and the solution was added dropwise to the first solution. The reaction mixture was stirred at room temperature for 7 days. Afterwards all volatiles were evaporated in vacuo and the residue recrystallized via vapor diffusion of pentane on a concentrated solution in THF. The crystals were filtered off, washed with pentane and dried in vacuum. Yield: 85 mg (colorless microcrystals, 36.0 %). ^1H NMR (δ in ppm, 300 MHz, $CDCl_3$, 298 K): 0.99 (t, 3H, CH$_2$CH_3), 1.03 (s, 9H, CCH_3), 1.41 (s, 9H, CCH_3), 1.55-1.66 (m, 1H, (OH)CCH_2), 1.68-1.80 (m, 1H, (OH)CCH_2), 2.96-3.04 (m, 2H, PCH_2), 4.01-4.14 (m, 1H, (OH)CH), 6.04 (dd, $^3J_{P-H}$ = 14.7 Hz, $^4J_{H-H}$ = 2.5 Hz, 1H, H5), 7.34-7.41 (m, 2H, Ar-H), 7.42 (d, 1H, $^4J_{H-H}$ = 2.7 Hz, H3), 7.47-7.54 (m, 6H, Ar-H), 7.57-7.64 (m, 2H, Ar-H), 8.06 (br, 1H, OH). $^{13}C\{^1H\}$ NMR (δ in ppm, 75 MHz, $CDCl_3$, 298 K): 10.3 (s, CH$_2$CH_3), 29.4 (s, CCH_3), 31.4 (s, CCH_3), 31.8 (d, $^3J_{P-C}$ = 16.4 Hz, (OH)CCH_2), 34.0 (d, $^4J_{P-C}$ = 1.5 Hz, CCH$_3$), 35.2 (d, $^4J_{P-C}$ = 2.4 Hz, CCH$_3$), 37.3 (d, $^1J_{P-C}$ = 57.8 Hz, PCH$_2$), 66.1 (d, $^2J_{P-C}$ = 3.8 Hz, (OH)C), 100.3 (d, $^1J_{P-C}$ = 96.8 Hz, C6), 122.8 (d, $^1J_{P-C}$ = 88.6 Hz, C$_{i-Ph}$), 126.9 (d, $^1J_{P-C}$ = 84.8 Hz, C$_{i-Ph}$),

127.5 (d, $^2J_{P-C}$ = 13.0 Hz, C5), 129.3 (d, $^3J_{P-C}$ = 10.6 Hz, C$_{m-Ph}$), 129.4 (d, $^3J_{P-C}$ = 8.6 Hz, C$_{m-Ph}$), 131.0 (d, $^4J_{P-C}$ = 2.4 Hz, C3), 132.6 (d, $^2J_{P-C}$ = 8.7 Hz, C$_{o-Ph}$), 132.7 (s, C$_{p-Ph}$), 132.8 (d, $^3J_{P-C}$ = 2.9 Hz, C$_{p-Ph}$), 133.0 (d, $^2J_{P-C}$ = 9.6 Hz, C$_{o-Ph}$), 134.1 (d, $^3J_{P-C}$ = 14.9 Hz, C4), 140.9 (d, $^3J_{P-C}$ = 8.2 Hz, C2), 173.7 (d, $^2J_{P-C}$ = 4.8 Hz, C1). ^{31}P{^{1}H} NMR (δ in ppm, 162 MHz, CDCl$_3$, 298 K): 18.8. UV-Vis (CHCl$_3$): λ_{max}= 345 nm (ε = 5.69 * 10^3 dm^3 mol^{-1} cm^{-1}).

2,4-di-tert-butyl-6-((2-hydroxy-2-phenylethyl)diphenylphosphonio)phenolate (**2c**, C$_{34}$H$_{39}$O$_2$P)

Synthesis was carried out in the same way as described for **2b**, using styrene oxide (61 mg, 0.51 mmol, 1 eq.). The residue obtained after evaporation of volatiles was recrystallized from a hot toluene/THF mixture. Yield: 124 mg (orange solid, 47.6 %). ^{1}H NMR (δ in ppm, 300 MHz, CDCl$_3$, 298 K): 1.11 (s, 9H, CCH_3), 1.51 (s, 9H, CCH_3), 3.15-3.29 (m, 1H, CH_2), 3.34-3.52 (m, 1H, CH_2), 5.29 (dd, 1H, $^3J_{H-H}$ = 12.4, 9.3 Hz, CH), 6.15 (dd, $^3J_{P-H}$ = 14.7 Hz, $^4J_{H-H}$ = 2.3 Hz, 1H, H5), 7.28-7.43 (m, 5H, Ar-H), 7.45-7.57 (m, 5H, Ar-H), 7.58-7.76 (m, 6H, Ar-H), 8.80 (br, 1H, OH). ^{13}C{^{1}H} NMR (δ in ppm, 75 MHz, CDCl$_3$, 298 K): 29.3 (s, CCH$_3$), 31.4 (s, CCH$_3$), 34.0 (d, $^4J_{P-C}$ = 1.1 Hz, CCH$_3$), 35.2 (d, $^4J_{P-C}$ = 2.1 Hz, CCH$_3$), 40.7 (d, $^1J_{P-C}$ = 53.8 Hz, PCH$_2$), 67.7 (d, $^2J_{P-C}$ = 3.8 Hz, (OH)C), 100.4 (d, $^1J_{P-C}$ = 96.5 Hz, C6), 122.4 (d, $^1J_{P-C}$ = 88.9 Hz, C$_{i-Ph}$), 125.8 (s, Ar-C), 126.5 (d, $^1J_{P-C}$ = 84.5 Hz, C$_{i-Ph}$), 127.4 (s, C5), 127.6 (s, Ar-C), 128.7 (s, Ar-C), 129.2 (d, $^3J_{P-C}$ = 11.3 Hz, C$_{m-Ph}$), 129.5 (d, $^3J_{P-C}$ = 12.4 Hz, C$_{m-Ph}$), 131.2 (d, $^4J_{P-C}$ = 1.9 Hz, C3), 132.5 (d, $^2J_{P-C}$ = 8.5 Hz, C$_{o-Ph}$), 132.7 (d, $^4J_{P-C}$ = 2.8 Hz, C$_{p-Ph}$), 133.0 (d, $^4J_{P-C}$ = 3.0 Hz, C$_{p-Ph}$), 133.0 (d, $^2J_{P-C}$ = 9.6 Hz, C$_{o-Ph}$), 134.5 (d, $^3J_{P-C}$ = 15.1 Hz, C4), 141.0 (d, $^3J_{P-C}$ = 7.8 Hz, C2), 145.1 (d, $^3J_{P-C}$ = 15.7 Hz, (OH)CHC_{Ar}), 173.6 (d, $^2J_{P-C}$ = 5.0 Hz, C1). ^{31}P{^{1}H} NMR (δ in ppm, 162 MHz, CDCl$_3$, 298 K): 18.3. UV-Vis (CHCl$_3$): λ_{max}= 345 nm (ε = 5.34 * 10^3 dm^3 mol^{-1} cm^{-1}).

2,4-di-tert-butyl-6-((2-hydroxy-3-phenoxypropyl)diphenylphosphonio)phenolate (**2d**, C$_{35}$H$_{41}$O$_3$P)

Synthesis was carried out in the same way as described for **2b**, using phenyl glycidyl ether (77 mg, 0.51 mmol, 1 eq). The obtained residue after evaporation of volatiles was recrystallized from hot toluene. Yield 162 mg (pale yellow crystals, 58.7 %). ^{1}H NMR (δ in ppm, 400 MHz, CDCl$_3$, 298 K): 1.05 (s, 9H, CCH_3), 1.44 (s, 9H, CCH_3), 2.95-9.10 (m, 1H, P-CH_2), 3.49-3.61 (m, 1H, P-CH_2), 3.84-3.94 (m, 1H, O-CH_2), 4.27-4.36 (m, 1H, O-CH_2), 4.42-4.56 (m, 1H, (OH)CH), 6.07 (dd, $^3J_{P-H}$ = 14.9 Hz, $^4J_{H-H}$ = 2.5 Hz, 1H, H5), 6.87-6.99 (m, 3H, Ar-H), 7.23-7.31 (m, 2H, Ar-H), 7.36-7.65 (m, 11H, Ar-H). ^{13}C{^{1}H} NMR (δ in ppm, 100 MHz, CDCl$_3$, 298 K): 29.3 (s, CCH$_3$), 31.4 (s, CCH$_3$), 34.0 (d, $^4J_{P-C}$ = 1.5 Hz, CCH$_3$), 34.8 (d, $^1J_{P-C}$ = 60.2 Hz, PCH$_2$), 35.3 (d, $^4J_{P-C}$ = 2.4 Hz, CCH$_3$), 63.9 (d, $^2J_{P-C}$ = 3.9 Hz, (OH)C), 70.9 (d, $^3J_{P-C}$ = 15.9 Hz, COPh), 100.7 (d, $^1J_{P-C}$ = 97.3 Hz, C6), 114.5 (s, OPh$_{ortho}$), 121.2 (s, OPh$_{para}$), 122.5 (d, $^1J_{P-C}$ = 88.1 Hz, C$_{i-Ph}$), 126.4 (d, $^1J_{P-C}$ = 86.2 Hz, C$_{i-Ph}$), 127.5 (d, $^2J_{P-C}$ = 12.5 Hz, C5), 129.3 (d, $^3J_{P-C}$ = 2.9 Hz, C$_{m-Ph}$), 129.4 (d, $^2J_{P-C}$ = 3.9 Hz, C$_{m-Ph}$), 129.7 (s, OPh$_{meta}$), 131.2 (d, $^4J_{P-}$

$_C$ = 2.4 Hz, C3), 132.6 (d, $^2J_{P-C}$ = 9.2 Hz, C$_{o-Ph}$), 132.8 (d, $^4J_{P-C}$ = 2.9 Hz, C$_{p-Ph}$), 132.9 (d, $^4J_{P-C}$ = 2.9 Hz, C$_{p-Ph}$), 133.1 (d, $^2J_{P-C}$ = 9.2 Hz, C$_{o-Ph}$), 134.6 (d, $^3J_{P-C}$ = 14.9 Hz, C4), 141.0 (d, $^3J_{P-C}$ = 7.7 Hz, C2), 158.2 (s, OPh$_{ipso}$), 173.4 (d, $^2J_{P-C}$ = 4.8 Hz, C1). ^{31}P{^{1}H} NMR (δ in ppm, 162 MHz, CDCl$_3$, 298 K): 18.7. UV-Vis (CHCl$_3$): λ$_{max}$ = 347 nm (ε = 5.75 * 10^3 dm^3 mol^{-1} cm^{-1}).

2-((3-butoxy-2-hydroxypropyl)diphenylphosphonio)-4,6-di-tert-butylphenolate (**2e**, C$_{33}$H$_{45}$O$_3$P)

2e was prepared analogously to **2b**, using butyl glycidyl ether (66 mg, 0.51 mmol, 1 eq.). The residue obtained after evaporation of volatiles was recrystallized by vapor diffusion of pentane on a concentrated solution in toluene. Yield: 89 mg (colorless solid, 33.5 %). ^{1}H NMR (δ in ppm, 400 MHz, CDCl$_3$, 298 K): 0.91 (t, $^3J_{H-H}$ = 7.3 Hz, 3H, CH$_2$C*H$_3$*), 1.03 (s, 9H, CC*H$_3$*), 1.33-1.40 (m, 2H, C*H$_2$*CH$_3$), 1.41 (s, 9H, CC*H$_3$*), 1.52-1.60 (m, 2H, C*H$_2$*CH$_2$), 2.85-2.98 (m, 1H, PC*H$_2$*), 3.38 (m, 1H, (OH)CC*H$_2$*), 3.43-3.49 (m, 3H, PC*H$_2$*' + OC*H$_2$*), 3.62-3.69 (m, 1H, (OH)CC*H$_2$*), 4.17-4.29 (m, 1H, (OH)C*H*), 6.04 (dd, $^3J_{P-H}$ = 14.7 Hz, $^4J_{H-H}$ = 2.7 Hz, 1H, H5), 7.37-7.45 (m, 3H, Ar-*H*), 7.46-7.52 (m, 4H, Ar-*H*), 7.53-7.64 (m, 4H, Ar-*H*), 8.23 (br, 1H, OH). ^{13}C{^{1}H} NMR (δ in ppm, 100 MHz, CDCl$_3$, 298 K): 14.1 (s, CH$_2$*C*H$_3$), 19.5 (s, *C*H$_2$CH$_3$), 29.4 (s, C*C*H$_3$), 31.4 (s, C*C*H$_3$), 32.0 (s, *C*H$_2$CH$_2$), 34.0 (d, $^4J_{P-C}$ = 1.2 Hz, *C*CH$_3$), 34.7 (d, $^1J_{P-C}$ = 59.7 Hz, P*C*H$_2$), 35.2 (d, $^4J_{P-C}$ = 2.4 Hz, *C*CH$_3$), 64.6 (d, $^2J_{P-C}$ = 4.3 Hz, (OH)*C*H), 71.3 (s, O*C*H$_2$), 74.5 (d, $^3J_{P-C}$ = 15.9 Hz, (OH)CH*C*O), 100.7 (d, $^1J_{P-C}$ = 97.8 Hz, C6), 123.3 (d, $^1J_{P-C}$ = 87.2 Hz, C$_{i-Ph}$), 126.7 (d, $^1J_{P-C}$ = 86.7 Hz, C$_{i-Ph}$), 127.5 (d, $^2J_{P-C}$ = 13.0 Hz, C5), 129.3 (d, $^3J_{P-C}$ = 11.6 Hz, C$_{m-Ph}$), 131.1 (d, $^4J_{P-C}$ = 2.4 Hz, C3), 132.6 (d, $^2J_{P-C}$ = 8.7 Hz, C$_{o-Ph}$), 132.8 (d, $^4J_{P-C}$ = 2.9 Hz, C$_{p-Ph}$), 133.2 (d, $^2J_{P-C}$ = 9.2 Hz, C$_{o-Ph}$), 134.3 (d, $^2J_{P-C}$ = 14.9 Hz, C4), 140.9 (d, $^4J_{P-C}$ = 7.7 Hz, C2), 173.6 (d, $^2J_{P-C}$ = 4.3 Hz, C1). ^{31}P{^{1}H} NMR (δ in ppm, 162 MHz, CDCl$_3$, 298 K): 18.9. UV-Vis (CHCl$_3$): λ$_{max}$ = 347 nm (ε = 5.77 * 10^3 dm^3 mol^{-1} cm^{-1}).

Data availability

All data that supports the findings of this study is available in the published article and/or the supporting information to this article.

Acknowledgment

References

[1] Kinjo N, Ogata M, Nishi K, Kaneda A, Dušek K. (1989) Adv Polym Sci 88:1 DOI: 10.1007/BFb0017963

[2] Pham HQ, Marks MJ in Ullmann's Encyclopedia of Industrial Chemistry (2005) Wiley-VCH. DOI: 10.1002/14356007.a09_547.pub2

[3] Karak N (2021) ACS Symp Ser 1385:1 DOI: 10.1021/bk-2021-1385.ch001

[4] Kim WG, Lee JY, Part KY (1993) J Polym Sci Part A: Polym Chem 31:633 DOI: 10.1002/app.1992.070441012

[5] Verma C, Olasunkanmi LO, Akpan ED, Quraishi MA, Dagdag O, El Gouri M, Sherif E-SM, Ebenso EE (2020) React Funct Polym 156:104741 DOI: 10.1016/j.reactfunctpolym.2020.104741

[6] Ryu JH, Choi KS, Kim WG (2005) J Appl Polym Sci 96:2287 DOI: 10.1002/app.21001

[7] Nagai A, Kokaku H, Ishii T (2002) J Appl Polym Sci 85:2335 DOI: 10.1002/app.10866

[8] Ogata M, Kinjo N, Eguchi S, Hozoji H, Kawata T, Sashima H (1992) J Appl Polym Sci 44:1795 DOI: 10.1002/app.1992.070441012

[9] Han S, Yoon HG, Suh KS, Kim WG, Moon TJ (2000) J Polym Sci Part A: Polym Chem 37:713 DOI: 10.1002/(SICI)1099-0518(19990315)37:6<713::AID-POLA6>3.0.CO;2-I

[10] Su C-C, Wei C-H, Yang C-C (2013) Ind Eng Chem Res 52:2528 DOI: 10.1021/ie302347r

[11] Tyberg CS, Shih P, Verghese N, Loos AC, Lesko J, Riffle JS (2000). Polymer 41:9033 DOI: 10.1016/S0032-3861(00)00298-6

[12] Li J, Liu Y, Sun Z, Zhang M, Hong, H Moon K-s, Wong C (2022) Chem Mater 34:3280 DOI: 10.1021/acs.chemmater.2c00067

[13] Boskin MJ, Denney DB (1959) Chem Ind 330 CAN 55:124747

[14] Speziale AJ, Bissing DE (1963) J Am Chem Soc 85:1888 DOI: 10.1021/ja00895a055

[15] Vedejs E, Fuchs PL (1973) J Am Chem Soc 95:822 DOI: 10.1021/ja00784a032

[16] Kalaiselvan A, Venuvanalingam P (2005) Tetrahedron Lett 46:4087 DOI: 10.1016/j.tetlet.2005.04.024

[17] Zhu Z, Espenson JH (1995) J Mol Catal A 103:87 DOI: 10.1016/1381-1169(95)00120-4

[18] Gable KP, Brown EC (2003) Synlett 2243 DOI: 10.1055/s-2003-42076

[19] Mitsudome T, Noujima A, Mikami Y, Mizugaki T, Jitsukawa K, Kaneda K (2010) Angew Chem Int Ed 49:5545 DOI: 10.1002/anie.201001055

[20] Heinicke JW (2024) Chem Eur J 30:e202302740 DOI: 10.1002/chem.202302740

[21] Büttner H, Steinbauer J, Wulf C, Dindaroglu M, Schmalz H-G, Werner T (2017) ChemSusChem 10:1076 DOI:10.1002/cssc.201601163

[22] Toda Y, Hashimoto K, Mori Y, Suga HJ (2020) Org Chem 85:10980 DOI:10.1021/acs.joc.0c01101

[23] Toda Y, Tanaka K, Matsuda R, Sakamoto T, Katsumi S, Shimizu M, Ito F, Suga H (2021) Chem Commun 57:3591 DOI:10.1039/d1cc00996f

[24] Toda Y, Kobayashi T, Hirai F, Yano T, Oikawa M, Sukegawa K, Shimizu M, Ito F, Suga H (2023) J Org Chem 88:9574 DOI: 10.1021/acs.joc.3c00988

[25] Edinger D, Fischer SM, Slugovc C (2024) *Macromol Chem Phys* 225:2300299 DOI: 10.1002/macp.202300299

[26] Noda H, Motokura K, Miyaji A, Baba t (2013) Adv Synth Catal 355:973 DOI: 10.1002/adsc.201300063

[27] He L-P, Mu H-L, Li B-X, Li Y-S (2010) J Polym Sci Part A: Polym Chem 48:311 DOI:10.1002/pola.23785

[28] Steiner MR, Schmallegger M, Donner L, Hlina JA, Marschner C, Baumgartner J, Slugovc C (2024) Beilstein J Org Chem 20:41 DOI: 10.3762/bjoc.20.6

[29] Cremer D, Kraka E (1985) J Am Chem Soc 107:3800 DOI: 10.1021/ja00299a009

[30] Morgan KM, Ellis JA, Lee J, Fulton A, Wilson SL, Dupart PS, Dastoori R (2013) J Org Chem 78:4303 DOI: 10.1021/jo4002867

[31] Heinicke J, Kadyrov R, Kindermann MK, Koesling M, Jones PG (1996) Chem Ber 129:1547 DOI: 10.1002/cber.19961291223

[32] Kim B, Storch G, Banerjee G, Mercado BQ, Castillo-Lora J, Brudvig GW, Mayer JM, Miller SJ (2017) J Am Chem Soc 139:15239 DOI: 10.1021/jacs.7b09176

[33] Haitham E, Yaccoubi F (2023) Phosphorus, Sulfur Silicon Relat. Elem. 198:354 DOI: 10.1080/10426507.2022.2150854

[34] Mannu A, Di Pietro, ME, Priola E, Baldino S, Sacchetti A, Mele A (2021) Res Chem Intermed 47:1663 DOI: 10.1007/s11164-020-04364-9

[35] Toda Y, Sakamoto T, Komiyama Y, Kikuchi A, Suga H (2017) ACS Catal 7:6150 DOI:10.1021/acscatal.7b02281

[36] Zhu X-F, Henry CE, Kwon OJ (2007) J Am Chem Soc 129:6722 DOI:10.1021/ja071990s

[37] Hamaguchi M, Iyama Y, Mochizuki E, Oshima T (2005) Tetrahedron Lett 46:8949 DOI:10.1016/j.tetlet.2005.10.086

[38] Heinicke J, Kadyrov R, Kindermann MK, Koesling M, Jones PG (1996) Chem Ber 129:1547 DOI: 10.1002/cber.19961291223

[39] Ehlers J-E, Rondan NG, Huynh LK, Pham H, Marks M, Truong TN (2007) Macromolecules 40:4370 DOI: 10.1021/ma070423m

[40] Sreejyothi P, Sarkar P, Dutta S, Das A, Pati SK, Mandal SK (2022) Chem Commun 58:9540 DOI: 10.1039/D2CC03549A

[41] Bloom SM, Buckler SA, Lambert RF, Merry EV (1970) J Chem Soc D 870 DOI: 10.1039/C29700000870

[42] Satpathi B, Dutta L, Ramasastry SSV (2019) Org Biomol Chem 17:1547 DOI: 10.1039/C8OB03106A

[43] Zhang J, Mück-Lichtenfeld C, Studer A (2023) Nature 619:506 DOI: 10.1038/s41586-023-06141-1

[44] Thevenon A, Cyriac A, Myers D, White AJP, Durr CB, Williams CKJ (2018) J Am Chem Soc 140:6893 DOI: 10.1021/jacs.8b01920

[45] Blessing RH (1995) Acta Crystallogr Sect. A: Found Crystallogr 51:33 DOI: 10.1107/s0108767394005726

[46] Sheldrick GM (2008) Acta Crystallogr Sect A: Found Crystallogr 64:112 DOI: 10.1107/s0108767307043930

[47] Momma K, Izumi F (2011) J Appl Crystallogr 2011, 44:1272 DOI: 10.1107/S0021889811038970